PHYSICAL REVIEW C VOLUME 27, NUMBER 1 JANUARY 1983

Comments

Comments are short papers which comment on papers of other authors previously published in **Physical Review C**. *Each Comment should state clearly to which paper it refers and must be accompanied by a brief abstract and keyword abstract.*

Separable potential analyses of coupled NN-$N\Delta$ scattering

W. M. Kloet* and J. A. Tjon
Institute for Theoretical Physics, Princetonplein 5, 3508 TA Utrecht, The Netherlands
(Received 24 June 1982)

The apparent differences between two analyses of the $^1D_2$ and $^3F_3$ nucleon-nucleon amplitudes by VerWest and the present authors are resolved. In both analyses dynamical poles are present in the scattering amplitude. These poles are associated with fixed left hand singularities.

[NUCLEAR REACTIONS Intermediate energy NN. Scattering theory. NN-$N\Delta$ coupled separable potentials.]

The resonancelike structure of the $^1D_2$ and $^3F_3$ nucleon-nucleon scattering amplitudes has been analyzed by means of a NN-$N\Delta$ coupled channel separable potential model independently by VerWest[1] and the present authors.[2,3] The aim of these analyses was to investigate the presence of dynamical poles in the $^1D_2$ and $^3F_3$ scattering amplitudes. The simplicity of the model allows for a straightforward analytic continuation of the amplitude into the complex energy or momentum plane, once the experimental data on the real axis have been fitted.

The results of VerWest[1] appear to be somewhat different from ours.[2,3] Searching for dynamical poles near the physical region we found one pole in the $^1D_2$ amplitude and two in the $^3F_3$ amplitude. All poles are close to the $N\Delta$ branch points. They have migrated there as a function of the coupling constants and originate for zero couplings from a nearby left hand singularity of the NN-$N\Delta$ transition potential v_{12}. VerWest finds fewer poles or none at all and makes a clear distinction between cases with and without resonances. In view of this, we have repeated the calculation of Ref. 1, and find that poles do exist caused by the same mechanism as discussed by us in Refs. 2 and 3. The unusual choice of delta parameters in Ref. 1, zero width, and a low mass of 1.200 GeV, causes a shift in the pole locations, away from the $N\Delta$ branch point. Actually, since for this parametrization the $N\Delta$ cut is on the real energy axis, some of the poles move into the upper complex energy plane and may therefore be overlooked. This is the major reason for the apparently different results of Ref. 1 and Refs. 2 and 3. Also, in one instance, a nearby pole in the lower complex energy plane was missed completely in Ref. 1. We proceed now to discuss the various fits to the $^1D_2$ and $^3F_3$ amplitudes given in Ref. 1. For each case we give the location as well as the origin of the dynamical poles resulting from our search.

The NN-$N\Delta$ coupled channel model of Ref. 1 is very similar to our two-body model discussed in the first part of Ref. 3. We note that the actual fitting in Refs. 2 and 3 was done with a somewhat more sophisticated three-body model. As mentioned above, the important difference between both two-body models is the treatment of the delta particle. VerWest chooses $M_\Delta = 1.200$ GeV mostly with zero width while we take $M_\Delta = 1.236 - 0.060i$ GeV. A minor difference is the choice of vertex functions $g_l(p)$. In Ref. 1 for the lth partial wave, the choice is

$$g_l(p) = p^l/(p^2+\mu_l^2)^{(l+2)/2} , \tag{1}$$

while in Refs. 2 and 3,

$$g_l(p) = p^l/(p^2+\mu_l^2)^{(l+1)/2} . \tag{2}$$

From now on we follow strictly the model and parametrization of Ref. 1. Because of $\Gamma_\Delta = 0$, the $N\Delta$ branch cut is on the physical axis. It causes a distinct cusp in the $^1D_2$ phase shift, but not in the $^3F_3$ phase. The parameters for the various $^1D_2$ and $^3F_3$ fits are given in Table I of Ref. 1. We will discuss solutions A and B for the $^1D_2$ phase and solutions A, B, and C for the $^3F_3$ phase. Instead of the laboratory kinetic energy T_L used in Ref. 1, we prefer to use the relative momentum $\hat{p}$ related to T_L by

$$T_L = 2\hat{p}^2/M . \tag{3}$$

In terms of this new variable the nucleon-nucleon amplitude has a branch cut due to the $N\Delta$ channel starting at $\hat{p} = 0.512$ GeV.

The parameters of solution A for the $^1D_2$ phase

given in Table I of Ref. 1 translate in our convention[2,3] into $\mu_1 = 0.272$ GeV and $\mu_2 = 0.473$ GeV for the masses in the two vertex functions of the separable coupled channel potential, and $\lambda_{11} = 0.013$, $\lambda_{12} = \lambda_{21} = 0.138$, $\lambda_{22} = 0.078$ for the channel coupling strengths. Following the procedure of Refs. 2 and 3 to search for poles in the nucleon-nucleon amplitude t_{11}, we find three poles. One pole is located at $\hat{p}_1 = 0.669 - 0.386i$ GeV ($T_L = 0.636 - 1.100i$ GeV) in the second $N\Delta$ sheet. This pole is mentioned in Ref. 1 and it is quite far from the real axis. We find a second pole at $\hat{p}_2 = 0.546 + 0.230i$ GeV ($T_L = 0.522 + 0.535i$ GeV) in the second $N\Delta$ sheet. This pole is somewhat closer to the physical region, but in the upper $\hat{p}$ plane, and it was ignored in Ref. 1. Since both $\hat{p}_1$ and $\hat{p}_2$ are relatively far from the physical region we mention still a third pole at $\hat{p}_3 = 0.152 - 0.199i$ GeV ($T_L = -0.016 - 0.129i$ GeV) in the first $N\Delta$ sheet. The location of the poles in the complex $\hat{p}$ plane is given in Fig. 1. The open triangle denotes $\hat{p}_1$, the solid triangle stands for $\hat{p}_2$, and $\hat{p}_3$ is represented by the open square. The origin of these dynamical poles can be traced by reducing subsequently λ_{11}, λ_{22}, and λ_{12} to zero and study the trajectory of each pole.[2,3] This pole movement is shown in Fig. 1 where solid curves are in the first $N\Delta$ sheet and dashed curves are in the second $N\Delta$ sheet. Each trajectory, in principle, is divided into three segments. Each segment is labeled (space allowing) by the coupling constant λ_{ij} that is varied along the segment. The poles at $\hat{p}_1$ and $\hat{p}_3$ originate for $\lambda_{11} = \lambda_{12} = \lambda_{21} = \lambda_{22} = 0$ from a fixed singularity of the NN potential v_{11} located at $\hat{p} = -i\mu_1$. The pole at $\hat{p}_2$ originates from a fixed singularity of the transition potential v_{12} at $p_R = -i\mu_2$ ($\hat{p} = 0.185$ GeV). The variable

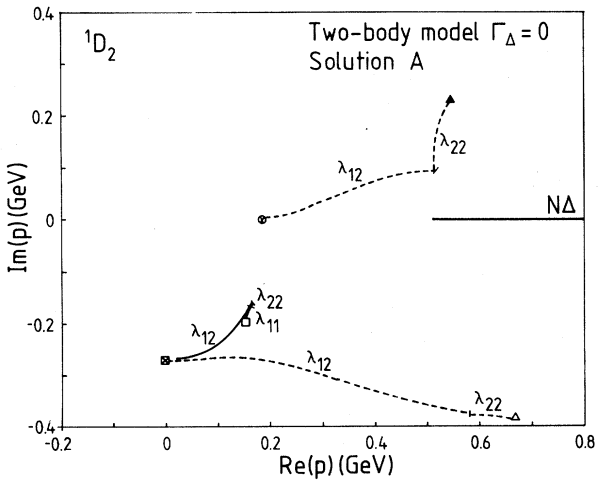

FIG. 1. Pole trajectories for solution A for the $^1D_2$ phase in the complex $\hat{p}$ plane. Dynamical poles are represented by Δ, ▲, and □. Left hand singularities are at ⊗ for v_{12} and at ⊠ for v_{11}. For further explanation see text.

p_R is the $N\Delta$ relative momentum defined by

$$p_R^2 = [s - (M_\Delta + M)^2][s - (M_\Delta - M)^2]/(4s) \quad . \tag{4}$$

In the more realistic three-body model also discussed in Refs. 2 and 3 it is the pole of the type $\hat{p}_2$ that is much closer to the physical region. It is usually near the $N\Delta$ branch point which, for finite delta width, is about 50 MeV below the real $\hat{p}$ axis. The poles $\hat{p}_1$ and $\hat{p}_3$ tend to be much further away from the real axis. We note that in the present case the effect on the real axis of all these poles is very weak because they are far away.

Solution B for the $^1D_2$ phase corresponds to $\mu_1 = 0.282$ GeV, $\mu_2 = 1.222$ GeV, $\lambda_{11} = 0.018$, $\lambda_{12} = \lambda_{21} = 0.374$, $\lambda_{22} = -0.929$. We find dynamical poles at $\hat{p}_1 = 0.515 - 0.580i$ GeV ($T_L = -0.152 - 1.272i$ GeV) in the second $N\Delta$ sheet, at $\hat{p}_2 = 0.424 + 0.122i$ GeV ($T_L = 0.351 + 0.220i$ GeV) in the second $N\Delta$ sheet and at $\hat{p}_3 = 0.159 - 0.201i$ GeV ($T_L = -0.032 - 0.136i$ GeV) in the first $N\Delta$ sheet. All poles are far away from the physical region and were ignored in Ref. 1. The location of the poles is indicated in Fig. 2 by an open triangle ($\hat{p}_1$), a solid triangle ($\hat{p}_2$), and an open square ($\hat{p}_3$). The poles $\hat{p}_2$ and $\hat{p}_3$ originate for zero coupling constants from a left hand singularity of v_{11} at $\hat{p} = -i\mu_1$. The pole at $\hat{p}_1$ originates from a fixed singularity of v_{12} at $\hat{p} = -1.067i$ GeV ($p_R = -i\mu_2$). This can be seen from the respective pole trajectories in Fig. 2. The fixed singularity of v_{12} in solution B is much farther away (and on the nega-

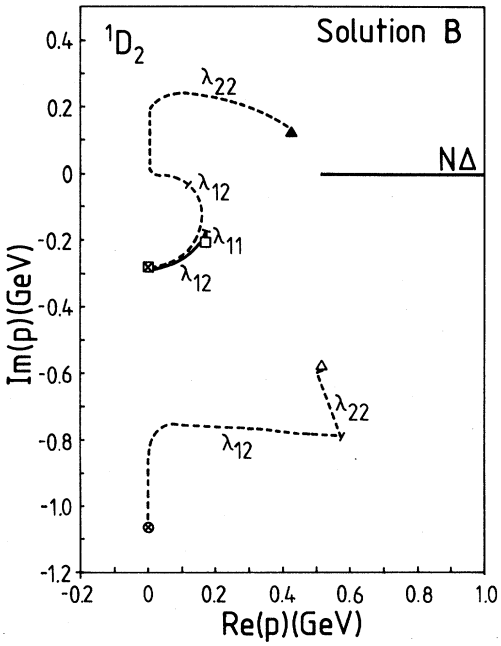

FIG. 2. Pole trajectories for solution B for the $^1D_2$ phase in the complex $\hat{p}$ plane. Symbols for the various poles are the same as in Fig. 1. For further explanation see text.

tive imaginary $\hat{p}$ axis) than for solution A where it is on the positive real $\hat{p}$ axis. This is due to the unusually large value of μ_2, which in realistic models should be of the order of a few hundred MeV. Consequently, in solution B the pole that emerges from the v_{12} singularity stays far away from the $N\Delta$ branch point and the nearest dynamical pole $\hat{p}_2$ actually is associated with a fixed singularity of v_{11}.

In the fits to the ${}^3F_3$ amplitude in Refs. 2 and 3 we find that two dynamical poles emerge from the fixed v_{12} singularity and both come close to the $N\Delta$ branch point. In Ref. 1 for solution A, only one pole is found and for solution B no pole at all. Part of this discrepancy arises since, because of the zero width of the delta in Ref. 1, one of the two poles remains above the $N\Delta$ cut in the upper $\hat{p}$ plane and is therefore ignored in Ref. 1. However, the second pole in solution B is in the lower $\hat{p}$ plane, rather close to the $N\Delta$ cut, and should not be ignored *ab initio*.

Our specific results for solution A for the ${}^3F_3$ phase corresponding to $\mu_1=0.418$ GeV, $\mu_2=0.146$ GeV, $\lambda_{11}=0.196$, $\lambda_{12}=\lambda_{21}=0.093$, $\lambda_{22}=0.030$ are shown in Fig. 3. From the fixed v_{12} singularity at $\hat{p}=0.490$ GeV ($p_R=-i\mu_2$), two dynamical poles emerge. One pole (open triangle) is located at $\hat{p}_1=0.559-0.141i$ GeV ($T_L=0.623-0.336i$ GeV) in the second $N\Delta$ sheet. This pole is mentioned in Ref. 1. The second pole (solid triangle) is found at $\hat{p}_2=0.594+0.086i$ GeV ($T_L=0.736+0.218i$ GeV), also in the second $N\Delta$ sheet.

Solution B for ${}^3F_3$ has parameters $\mu_1=0.416$ GeV, $\mu_2=0.584$ GeV, $\lambda_{11}=0.216$, $\lambda_{12}=\lambda_{21}=0.318$, $\lambda_{22}=-0.509$. It has two poles at $\hat{p}_1=0.526-0.045i$ GeV ($T_L=0.585-0.101i$ GeV) and at $\hat{p}_2=0.549+0.046i$ GeV ($T_L=0.637+0.108i$ GeV), respectively. Both poles are in the second $N\Delta$ sheet. The positions are given in Fig. 4 by the open triangle for $\hat{p}_1$ and the solid triangle for $\hat{p}_2$. The location of the two poles near the $N\Delta$ branch cut is not essentially different from our own fits to the ${}^3F_3$ phase in Refs. 2 and 3. Reducing subsequently λ_{11}, λ_{22}, and λ_{12} to zero gives the pole trajectories. For zero coupling the trajectories originate at fixed singularities of v_{12} at $\hat{p}=\pm 0.294i$ GeV or $p_R=-i\mu_2$. These singularities are labeled B in Fig. 4.

Solution C for the ${}^3F_3$ phase corresponds to $\mu_1=0.317$ GeV, $\mu_2=0.054$ GeV, $\lambda_{11}=0.039$, $\lambda_{12}=\lambda_{21}=0.018$, $\lambda_{22}=0.008$. Poles are found at $\hat{p}_1=0.589-0.044i$ GeV ($T_L=0.735-0.1101i$ GeV) and $\hat{p}_2=0.590+0.030i$ GeV ($T_L=0.740+0.075i$ GeV) both in the second $N\Delta$ sheet. The pole location and the pole movement as a function of the coupling parameters are given in Fig. 4. The open square stands for $\hat{p}_1$ and the solid square denotes $\hat{p}_2$. The fixed singularity of v_{12}, labeled C, is very close to the $N\Delta$ branch point, because μ_2 is extremely small.

It is remarkable that the two solutions B and C, which have very different locations of the left hand singularities of v_{12} given by $p_R=-i\mu_2$, end up with dynamical poles that are relatively close. The phase shift for solution C differs[1] from the phase shift for solution B above $T_L=800$ MeV, but this difference is not essential. In both cases dynamical poles exist equally far from the real $\hat{p}$ axis.

The pole location for the various fits are summarized in Table I. Only three of these poles were quoted in Ref. 1. They are indicated by an asterisk in the last column. There is no reason to omit (as was done in Ref. 1) the poles in the upper complex $\hat{p}$ plane, be-

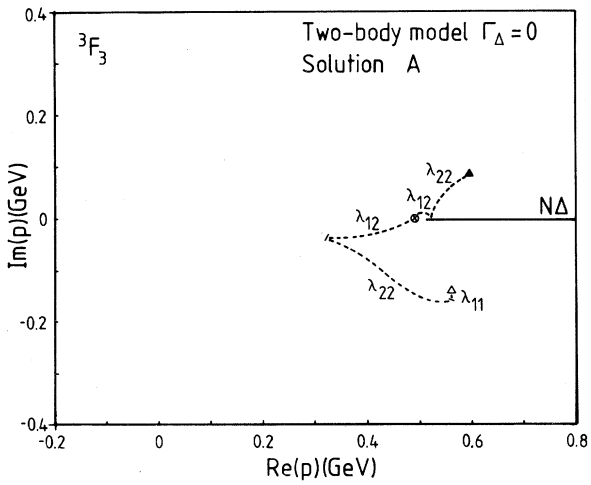

FIG. 3. Pole trajectories for solution A for the ${}^3F_3$ phase in the complex $\hat{p}$ plane. Dynamical poles are represented by Δ and $\blacktriangle$. The left hand singularity of v_{12} is at $\otimes$. For further explanation see text.

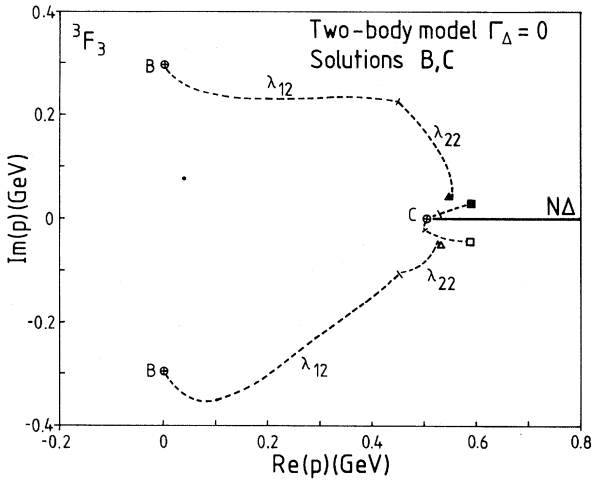

FIG. 4. Pole trajectories for solutions B and C for the ${}^3F_3$ phase in the complex $\hat{p}$ plane. For solution B dynamical poles are at Δ and $\blacktriangle$, and the left hand singularities of v_{12} are at $\otimes$, labeled B. For solution C dynamical poles are at $\square$ and $\blacksquare$, and the fixed singularity of v_{12} is at $\otimes$, labeled C. For further explanation see text.

TABLE I. Pole locations in complex $\hat{p}$ plane for the various fits. The poles that are quoted in Ref. 1 are indicated by an *.

	$\hat{p}$ (MeV)	$N\Delta$ sheet	Quoted in Ref. 1
$^1D_2$-solution A	$0.669-0.386i$	2	*
	$0.546+0.230i$	2	
	$0.152-0.199i$	1	
$^1D_2$-solution B	$0.515-0.580i$	2	
	$0.424+0.122i$	2	
	$0.159-0.201i$	1	
$^3F_3$-solution A	$0.559-0.141i$	2	*
	$0.594+0.086i$	2	
$^3F_3$-solution B	$0.526-0.045i$	2	
	$0.549+0.046i$	2	
$^3F_3$-solution C	$0.589-0.044i$	2	*
	$0.590+0.030i$	2	

cause in a more realistic model they may have moved into the lower $\hat{p}$ plane. Of course, for the present parametrization all poles in the $^1D_2$ solutions remain relatively far from the physical region, but not so for the $^3F_3$ solutions. A more serious omission, however, is the pole in the lower $\hat{p}$ plane in solution B for the $^3F_3$ phase. The presence of this pole means that solutions B and C for the $^3F_3$ phase are not essentially different with respect to the singularity structure. Both solutions display dynamical poles relatively close to the real axis.

With the above discussion the differences between the results quoted in Ref. 1 and the calculation of Refs. 2 and 3 have been resolved. In all cases of fits to the $^1D_2$ and $^3F_3$ amplitudes, dynamical poles are found and they are associated with fixed left hand singularities. A coupled NN-$N\Delta$ channel model with a fixed mass Δ particle only gives a crude description of medium energy nucleon-nucleon scattering. It may lead to substantial shifts in the location of dynamical poles. Within this kind of approach a model where the delta is treated as a pion-nucleon state[2,3] may give a more accurate description.

One of the authors (W.M.K.) is grateful to the Stichting Fundamenteel Onderzoek der Materie for support, and to the Insitute for Theoretical Physics at Utrecht for its hospitality. This work was supported in part by the National Science Foundation under Grant No. PHY-79-02961-02.

*On leave from the Department of Physics and Astronomy, Rutgers University, New Brunswick, N.J. 08903.

[1]B. J. VerWest, Phys. Rev. C 25, 482 (1982).
[2]W. M. Kloet and J. A. Tjon, Phys. Lett. 106B, 24 (1981).
[3]W. M. Kloet and J. A. Tjon, Nucl. Phys. A392, 271 (1983).